Publication Year	1994
Acceptance in OA@INAF	2023-02-03T16:31:14Z
Title	Metal enrichment in elliptical galaxies and globular clusters through the study of iron and H-beta spectral indices
Authors	BUZZONI, Alberto; Mantegazza, L.; Gariboldi, G.
DOI	10.1086/116873
Handle	http://hdl.handle.net/20.500.12386/33158
Journal	THE ASTRONOMICAL JOURNAL
Number	107

1994AJ....107..513B

THE ASTRONOMICAL JOURNAL VOLUME 107, NUMBER 2 FEBRUARY 1994

METAL ENRICHMENT IN ELLIPTICAL GALAXIES AND GLOBULAR CLUSTERS THROUGH THE STUDY OF IRON AND Hβ SPECTRAL INDICES[1]

ALBERTO BUZZONI
Osservatorio Astronomico de Brera, Via Brera, 28 20121 Milano, Italy
Electronic mail: buzzoni@astmin.mi.astro.it

LUCIANO MANTEGAZZA
Dip. di Fisica Nucleare e Teorica, Università di Pavia, Via Bassi, 6 27100 Pavia, Italy
Electronic mail: mantegazza@astmin.mi.astro.it

GIORGIO GARIBOLDI
Osservatorio Astronomico di Brera, Via Brera, 28 20121 Milano, Italy
Received 1992 October 12; revised 1993 June 22

ABSTRACT

Chemical evolution of elliptical galaxies and globular clusters is addressed through a combined study of the iron indices at 5270 and 5335 Å, and of the Hβ line strength. The observational database of 74 standard stars (both dwarfs and giants) referred to in a previous paper {Buzzoni *et al.* [AJ, 103, 1814, (1992)]} complemented with the data of Faber *et al.* [ApJS, 57, 711 (1985)] and Gorgas *et al.* [ApJS, 86, 153 (1993)] allowed us to explore here Fe and Hβ index dependence on stellar temperature, gravity, and metallicity. The derived fitting functions were then included into Buzzoni's [ApJS, 71, 817 (1989)] code for population synthesis in order to derive expected integrated indices for simple stellar populations and compare with observations. Partition of metals in the current chemical mix of galaxies and globulars has been constrained supporting the claim that light α elements might be enhanced in the globular cluster metal-poor population. An alternative conclusion resting on the standard framework with [α/Fe]=0 would require a systematically larger age, about 18–20 Gyr. Iron and magnesium in ellipticals are found in average solar but a systematic trend of [Mg/Fe] vs global metallicity does exist with iron more deficient with respect to magnesium at high Z. We conclude that this effect might indicate that Fe abundance per unit mass in the galaxies is constant (suggesting a constant rate per unit mass of SN I events) while light metals supplied by SNe II should have been more effectively enriched with increasing galactic total mass.

1. INTRODUCTION

The study of spectral indices is revealing a potentially powerful tool to investigate in fine detail the overall evolutionary status of stellar systems. Integrated spectral lines in fact collect light selectively from stars in an aggregate, and can effectively single out the stellar contribution to the total spectral energy distribution from a specific range in temperature, gravity, and metallicity.

There is a direct link between effective physical parameters of stars contributing a narrow-band index and the distinctive properties of the parent stellar population in a cluster. Measuring the effective temperature of warmer stars in the main sequence (MS) of a population for example we get hints about its age and metallicity, while a general knowledge of the gravity distribution of stars is a clue for deriving the present mass distribution and the initial mass function (IMF).

Once metallicity effects in a stellar population can be properly singled out through a combined study of spectral features it would be possible in principle to get a rather accurate analysis of the primeval nucleosynthesis products and the subsequent metal enrichment in stars. As far as we consider in more detail the question it is clear that the original assumption that "metals" would consist of a homogeneous set of elements with fixed relative partition is nothing else than a useful but too simplified statement. It is well established in fact that the Big Bang provided hydrogen and helium while intermediate and heavy elements came from stellar burning and from supernovae, respectively. The envisaged scenario is therefore too complex to firmly conclude that metal enrichment in different stellar systems proceeded in the same way.

In particular, two problems might be addressed in this concern. The first one deals with the observational evidence that oxygen is enhanced with respect to iron in Population II stars in the Galaxy (Wheeler *et al.* 1989; Bessell *et al.* 1991; Sneden *et al.* 1991; Gratton 1992). This effect might be regarded as a sign for a differentiated role of supernovae in modulating chemical evolution. A similar problem might also concern elliptical galaxies as from a preliminary analysis magnesium and iron might be decoupled in concurring to the chemical mix of those stellar populations (Worthey *et al.* 1992).

A pioneering work toward a systematic definition and

[1]Based on observations made at the European Southern Observatory (ESO) La Silla, Chile.

 0004-6256/94/107(2)/513/17/$0.90 © 1994 Am. Astron. Soc.

© American Astronomical Society • Provided by the NASA Astrophysics Data System

1994AJ....107..513B

application of spectral indices in the study of stellar populations is that of Spinrad & Taylor (1969), and Taylor (1970), who derived metal abundances in Galactic stars through a combined analysis of a wide set of indices spanning the stellar spectrum from the ultraviolet to the near infrared. This work was then the basis for a first effective attempt to use population synthesis techniques for modeling external galaxies like M31, M32, and M81 (Spinrad & Taylor 1971).

Since then, an increasing number of studies focused on this field, making clear that once coupled with accurate models for population synthesis, the observation of the line strength in integrated spectra of galaxies could be the most viable alternative to investigate their unresolved stellar populations as effectively as we can, e.g., for the Galactic globular clusters through their color–magnitude (cm) diagrams.

Ultraviolet spectral indices have been carefully explored in Galactic stars by Rose (1984, 1985a,b) and Rose & Tripicco (1984), and a direct extension of those results to the case of M32 and to the study of elliptical galaxies was attempted by Rose (1985c), and Boulade *et al.* (1988).

On the opposite side, infrared indices have been widely investigated by Frogel and colleagues with special care to the two CO and H_2O features about 2 μm (Baldwin *et al.* 1973; Baldwin *et al.* 1973). Aperture photometry in the CO and H_2O bands of elliptical galaxies and globular clusters was carried out by Aaronson *et al.* (1978), and Frogel *et al.* (1978), and discussed in the more general interpretative framework by Frogel *et al.* (1980) for early type galaxies, and by Frogel (1985) for spiral galaxies.

Faber and colleagues underwent a systematic analysis of stellar spectra in the visual range specifically aimed at modeling narrow-band indices in galaxies through population synthesis models (Faber 1973; Faber & French 1980; Burstein *et al.* 1984; Faber *et al.* 1985; Worthey *et al.* 1992; Worthey 1992; Gorgas *et al.* 1993).

Although all these studies greatly contributed to refine our knowledge of the behavior of some relevant spectral features in stars, nevertheless we believe that an intervening weak point in common is always a lack of an adequate link to models for population synthesis in order to match galaxies and other stellar systems with a better accuracy. Complete stellar isochrones are in fact necessary in order to properly include in the computation luminous stars from any evolutionary phase that could contribute to the integrated spectral energy distribution. Moreover, the relative weight of stars in the different phases should be proportional to the actual relative lifetimes according to the prescriptions of the fuel consumption theorem (Renzini & Buzzoni 1986).

This study intends therefore to carry on a more accurate analysis of the spectral indices in stellar systems securing on more solid bases the comparison of observations with models for evolutionary population synthesis (Buzzoni 1989). It is our second step along the project already undergone with the study of the magnesium Mg_2 index (Buzzoni *et al.* 1992, hereafter referred to as Paper I).

Here, we will include three more indices among the most popular ones defined by Faber *et al.* (1985), that is the two iron features at 5270 and 5335 Å (hereafter referred to as Fe52 and Fe53, respectively), and the hydrogen Hβ at 4861 Å. We will show in particular that a combined analysis of the line strengths of metals and hydrogen provides a powerful tool for an in-depth investigation of the chemical properties of stars in early type galaxies and globular clusters.

In the following, we will arrange our analysis presenting the observational database in Sec. 2, and deriving there an accurate calibration of the indices for accounted stars. The fitting functions derived from stars will be included in the evolutionary population synthesis code of Buzzoni (1989) deriving in Sec. 3 synthetic indices for a wide grid of theoretical simple stellar populations (SSPs). Comparison with available observations of elliptical galaxies and globular clusters will be performed in Sec 4 discussing in more detail some relevant questions dealing with the chemical evolution in these stellar systems. Our conclusions will be finally summarized in Sec. 5.

2. FITTING STAR INDICES

One possible way to obtain synthetic spectral indices for model stellar populations relies on the determination of fitting functions giving (possibly in an analytical form) the behavior of a feature vs the three main physical parameters of stars, i.e., temperature, gravity, and metallicity.

As well recognized, fitting functions can hardly be derived from a purely theoretical study of model stellar atmospheres due to our still incomplete knowledge of chemical opacities and other leading parameters modulating the shape and strength of spectral lines (see, e.g., Kurucz 1992 for an updating discussion of this problem).

In the alternative, one practicable way relies on the direct observations of Galactic standard stars in the solar neighborhood for which we can retrieve in some way intrinsic physical parameters. Operationally, this is by far the more simple and useful solution but, as discussed in Paper I and by Gorgas *et al.* (1993), it is not free from a potential biasing effect due to the fact that the derived empirical calibration implicitly rests on a solar partition of metals in the chemical mix.

In Paper I we were able to verify that such an assumption still holds for magnesium, and we concluded that it can be regarded as a fair tracer of the total metallicity in outer galaxies. However, it is clear that our statement cannot be automatically extended also to all other metal elements, and rather requires to be directly probed.

2.1 The Fe52 and Fe53 Indices

Fitting functions for Fe52 and Fe53 have been derived from the extended stellar sample of Paper I. Also in this case we retained the same criteria, selecting a stellar working sample more suitable for the synthesis of SSPs of intermediate and old age. Therefore, 74 stars of KM classes III–V were accounted, including for comparison also 130 field and cluster giants and dwarfs with reliable temperature, gravity, and metallicity from Faber *et al.* (1985) and

© American Astronomical Society • Provided by the NASA Astrophysics Data System

1994AJ....107..513B

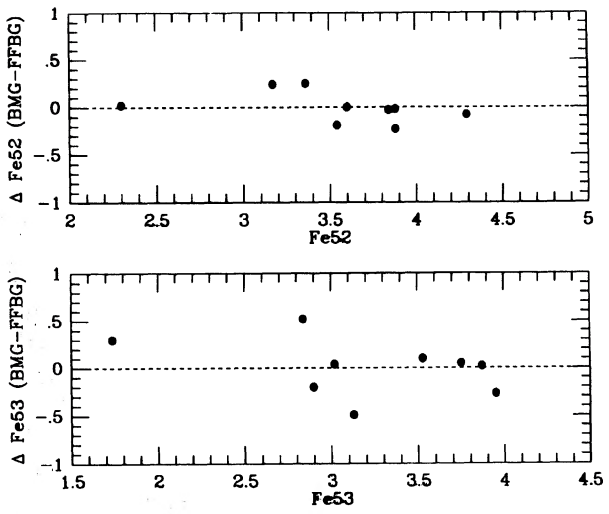

FIG. 1. Calibration residuals of Fe52 and Fe53 indices for the nine standard stars in common with Faber *et al.* (1985) (see Paper I for their HD identification). The scatter of the points is $\sigma_{Fe52} = \pm 0.16$ Å and $\sigma_{Fe53} = \pm 0.30$ Å.

Gorgas *et al.* (1993). As in Paper I, the reference source for stellar metallicity is the catalogue of Cayrel de Strobel *et al.* (1985).

Instrumental indices were obtained according to Burstein *et al.* (1984) and are expressed as pseudoequivalent width in Å of the features measured in the interval 5248.0–5286.75, and 5314.75–5353.50 Å for Fe52 and Fe53, respectively. The pseudocontinuum reference level was derived from both sides of the features [i.e. (5235.50–5249.25)Å + (5288.00–5319.25)Å for Fe52 and (5307.25–5317.25)Å + (5356.00–5364.75)Å for Fe53], and interpolated to the central wavelength of the features.

Nine stars in common with Faber *et al.* (1985) and well distributed in the index plane allowed us to translate to the standard system. This resulted in an offset in excess of 0.37 Å for both Fe52 and Fe53 with no significant systematic trends in the residuals. Standard values for both indices were therefore obtained by subtracting the offset to the instrumental output. As shown in Fig. 1, the standard system has been reproduced at 1 σ within ± 0.16 Å for Fe52, and ± 0.30 Å for Fe53. No supplementary correction was applied to the data; in particular, line broadening due to stellar rotational velocity was found to be negligible anyway (See Table 1a in Paper I). The final values of Fe52 and Fe53 indices for our whole stellar sample are reported in Table 1. In the table, stars are labeled with their HD number except the eight red dwarfs identified by their Gliese number and labeled GL.

Uncertainties in the indices can be derived from photon statistics according to Brodie & Huchra (1990) and result typically in ± 0.13 Å for both Fe52 and Fe53, at 1σ level.

TABLE 1. Observational sample.

Name	Fe52	Fe53	$H\beta$	Name	Fe52	Fe53	$H\beta$	Name	Fe52	Fe53	$H\beta$
1581	1.56	1.17	3.05	46407	2.75	1.82	1.62	102870	1.76	1.04	3.65
1835	2.63	1.83	2.83	47205	3.68	3.06	1.42	111631	3.97	4.56	−0.75
3443	2.42	1.96	2.08	50778	3.81	3.80	0.61	188510	0.51	0.17	1.91
10380	3.65	3.63	0.65	50877	5.61	5.35	2.31	189567	1.67	1.13	2.37
10700	2.20	1.62	1.68	56577	4.15	4.61	1.58	190248	3.09	2.15	2.61
13611	2.50	1.84	1.95	60219	1.75	0.73	4.41	191408	2.76	2.02	1.06
13974	1.65	1.26	2.11	62576	1.75	0.73	4.41	192310	3.87	2.90	1.30
14802	1.76	1.15	3.05	62644	2.49	1.92	2.23	192947	3.16	2.50	1.81
17925	4.02	3.14	1.50	63302	5.52	4.90	2.32	196378	1.08	0.60	3.22
18322	3.25	2.65	1.25	65699	3.18	2.33	2.11	203638	3.87	3.46	1.43
20630	2.56	1.81	2.63	69267	3.86	3.89	0.58	208776	1.58	1.09	3.17
20766	1.91	1.27	2.52	76151	2.46	1.64	2.73	209100	4.61	4.13	0.34
20794	2.17	1.74	2.06	83548	2.69	1.98	1.93	211391	3.29	2.53	1.93
20807	1.65	1.07	2.77	84810	3.40	2.37	3.34	212330	2.14	1.53	2.68
20894	2.62	1.86	1.96	84903	0.35	0.17	1.33	213009	3.13	2.51	2.03
22049	4.00	3.07	1.27	88218	1.65	0.97	2.83	215104	3.03	2.52	1.67
22484	1.64	1.04	3.24	88284	3.41	2.64	1.80	216437	2.38	1.63	3.08
30495	2.24	1.57	2.82	89388	4.30	4.14	1.29	216763	2.75	2.14	1.56
30562	2.21	1.83	3.32	91324	1.11	0.40	3.55	219615	2.08	1.63	1.50
32147	5.15	4.55	0.46	91805	2.55	1.82	1.82	221148	4.21	3.68	1.28
33793	3.15	2.70	−1.40	95272	3.35	2.70	1.57	225212	4.37	4.62	1.15
36395	3.04	3.19	0.32	95345	3.22	2.68	1.18	GL 229	3.32	3.18	0.05
37160	2.32	2.04	1.33	96918	4.21	1.23	3.71	GL 234	2.03	0.78	−11.57
37763	4.31	4.01	1.39	97907	3.61	3.36	1.27	GL 273	2.27	0.61	2.92
39091	1.91	1.30	3.19	98430	2.52	2.00	1.30	GL 488	4.53	4.61	−1.03
39364	2.32	2.02	1.31	99491	3.39	2.37	2.31	GL 551	0.91	−1.35	3.65
39523	3.58	3.13	1.63	100407	2.97	2.13	1.92	GL 673	4.49	4.79	−0.89
44033	3.56	4.27	0.67	102365	1.87	1.22	2.34	GL 699	1.16	0.91	2.07
45829	4.65	3.99	2.54	102634	1.65	1.01	4.10	GL 729	1.93	1.30	−0.47

© American Astronomical Society • Provided by the NASA Astrophysics Data System

1994AJ....107..513B

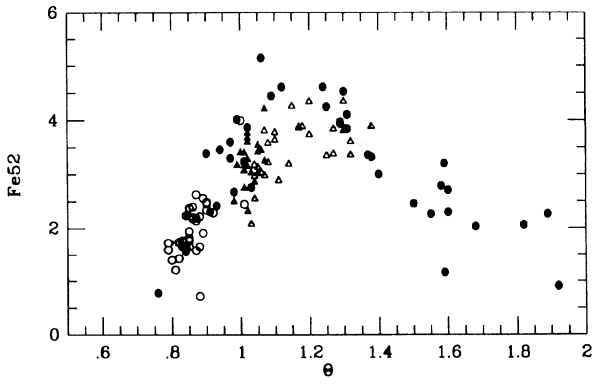

FIG. 2. Temperature dependence of Fe52. Displayed are 125 stars in the present working sample and in the Faber *et al.* (1985) and Gorgas *et al.* (1993) samples with [Fe/H] = ±0.25 (red dwarfs are included disregarding their [Fe/H]). Points are labeled according to their gravity in the bins log g=[1.5–2.5](△), [2.5–3.5](▲), [3.5–4.5](○), and [⩾4.5](●). The trend is clearly evident with the index increasing with decreasing temperature up to a maximum about $\Theta \sim 1.15$ ($T \sim 4300$ K), and then fading toward red dwarfs.

Once added in quadrature with the typical error for the Faber *et al.* (1985) standard stars (i.e., ~0.25–0.30 Å), this value can fully account for the variance in reproducing the standard system. This assures that photon statistics is

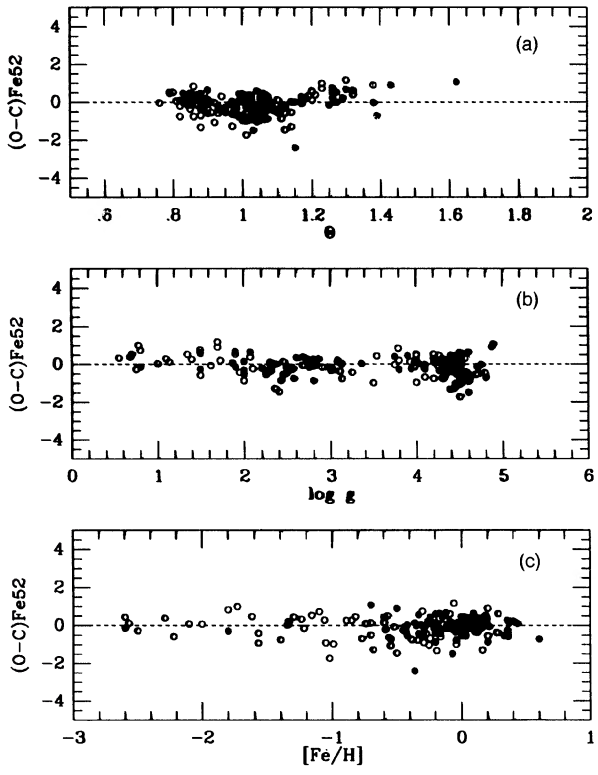

FIG. 3. (a)–(c) Residuals of Fe52 from fitting Eqs. (1)–(3) vs stellar temperature, gravity, and metallicity. Displayed are the 74 stars in the working sample (full dots) plus the 130 stars in the Faber *et al.* (1985) and Gorgas *et al.* (1993) samples (open dots). The scatter of our points is ±0.44 Å (±0.51 Å for the global sample of 204 points).

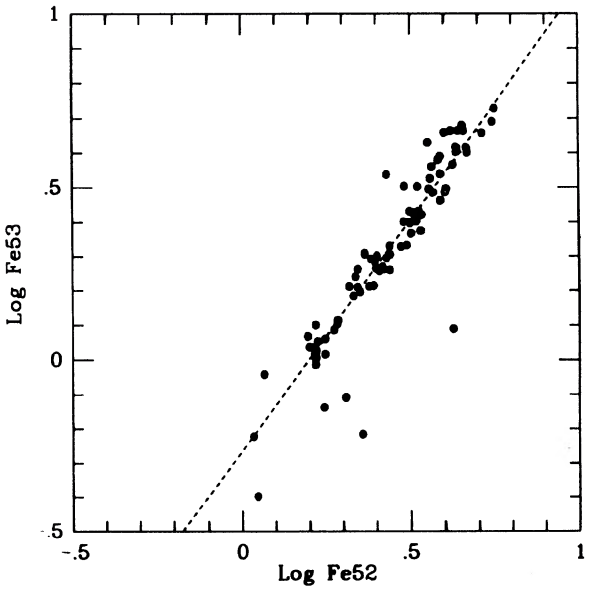

FIG. 4. Relationship between the two iron indices Fe52 and Fe53 in our complete sample of 87 standard stars of Table 1. The dashed line is the adopted relation log Fe53 = 1.34 log Fe52 − 0.264.

the main source of random error in our data.

A first sketch of the behavior of the iron indices with changing stellar spectral type can be derived from Fig. 2. Here, we displayed Fe52 vs the temperature parameter $\Theta \equiv 5040/T$ for all stars in our working sample and in the Faber *et al.* (1985) and Gorgas *et al.* (1993) samples with solar metallicity (red dwarfs are included disregarding their [Fe/H]). One clearly sees that the line strength is stronger with decreasing temperature reaching a maximum about 4300 K and then fading in the red dwarfs. This trend is substantially supported by the Gorgas *et al.* (1993) sample, also added in the figure. In order to remain free from any arbitrary assumption about the absolute temperature scale, in their original paper Gorgas *et al.* (1993) adopted $V-K$ instead of Θ as leading parameter in the fitting functions (see their Fig. 7a, for example). In our opinion this does not necessarily favor a more net discrimination of the index dependence on the physical parameters of the stars as $V-K$ itself is a function of stellar gravity and metallicity so that their fitting Eqs. (9) and (10) might be in fact redundant.

A good fit to Fe52 in our data can be performed considering the two index regimes at warm and cool temperatures. The maximum size the index can reach for different combinations of gravity and metallicity is found to be

$$\mathrm{Fe52_{MAX}} = 0.2 \log g + 1.15[\mathrm{Fe/H}] + 4.00. \quad (1)$$

Considering warm stars in the rising branch of Fig. 2 we have

$$\mathrm{Fe52} = 13.00\Theta + 0.53 \log g + 1.15[\mathrm{Fe/H}] - 11.50 \quad (2)$$

while the fading branch can be fitted by

$$\mathrm{Fe52} = -6.12\Theta + 0.118 \log g + 1.15[\mathrm{Fe/H}] + 11.00. \quad (3)$$

© American Astronomical Society • Provided by the NASA Astrophysics Data System

1994AJ....107..513B

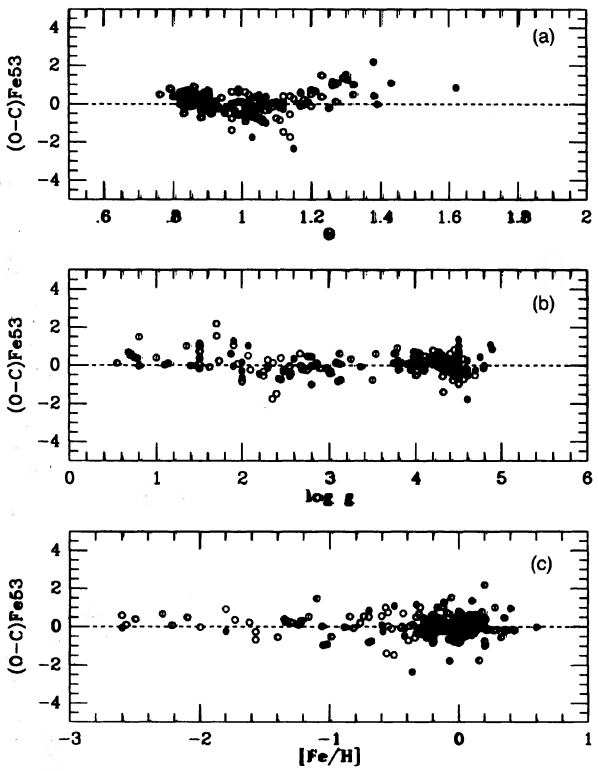

FIG. 5. (a)–(c) Residuals of Fe53 from adopted calibration. Points have the same meaning as in Fig. 3. The scatter is ±0.52 Å in our working sample and ±0.58 Å for the global sample of 204 points.

Operationally, the fitting value to be attributed to a given combination of Θ, log g, and [Fe/H] can be simply derived as Fe52=inf [Eq.(2), Eq.(3)].

Of course, the adopted fit is a simplification in favor of a more plain analytical representation of the data, still effective, however, in the relevant range for temperature, gravity, and metallicity of stars. The Θ−log g−[Fe/H] plane is not homogeneously populated by real stars, and therefore more attention has to be paid in order to optimize the fit according to the realistic combinations of the parameters.

The reliability of our fit can be checked with the help of Fig. 3 where we plotted the residuals from the stellar working sample both vs Θ, log g, and [Fe/H]. No systematic trends in the data are evident, and also the Faber *et al.* (1985) and Gorgas *et al.* (1993) samples are fairly well accounted by the fit. In particular, we can conclude that the assumed orthogonality between Θ, log g, and [Fe/H] in the fitting functions, although slightly relaxing the physical concern, is still a good representation of the data. The standard deviation of residuals is found to be $\sigma(O-C) = \pm 0.44$ Å mostly induced by the uncertainty in the adopted physical parameters of the stars.

The Fe53 index directly correlates to Fe52 as shown in Fig. 4. A simple fitting relation is

$$\log \mathrm{Fe53} = 1.34 \log \mathrm{Fe52} - 0.264. \quad (4)$$

TABLE 2. Fiducial super metal-rich stars.

Name	C85	C92	G93	T91	HK71
* 1835	.05	.21	—	—	—
10307	.12	.12	.12	—	—
10780	.36	.36	.36	—	—
* 18322	.20	.21	—	.17	−.25
19476	.12	.12	.22	.11	—
27371	.08	.08	.15	.08	−.05
27697	.06	.09	.15	.08	−.04
28307	.13	.08	.15	.08	−.04
* 30495	.10	.10	—	—	—
* 30562	.13	.13	.14	—	—
34411	.14	.18	.19	—	—
* 36395	.60	.60	—	—	—
* 37763	.35	.35	—	—	—
* 39523	.15	.15	—	.17	—
58207	.16	.16	−.10	−.19	−.31
72324	.32	.06	.17	−.21	−.03
75732	.13	.13	.13	—	—
85503	.07	.33	.46	—	.28
* 88284	.10	.10	—	.02	.13
88230	.28	.28	.28	—	—
* 95272	−.12	.10	−.06	−.05	−.22
*102634	.12	.12	—	—	—
*102870	.24	.19	.18	—	—
120136	.21	.18	.21	—	—
139669	.20	.20	−.10	—	−.59:
140573	.14	.20	.25	—	.19
145675	.27	.27	.27	—	—
184406	.16	.16	.22	.15	.08
186408	.14	.15	.14	—	—
187691	.12	.12	.12	—	—
*190248	.43	.30	—	—	—
*192947	.12	.12	—	.10	−.22
*203638	.35	.35	—	.37	—
*216437	.10	.10	—	—	—
* G229	.20	—	—	—	—
* G673	.40	—	—	—	—

C85 Cayrel de Strobel et al. (1985)
C92 Cayrel de Strobel et al. (1992)
G93 Gorgas et al. (1993)
T91 Taylor (1991)
HK71 Hansen and Kjaergaard (1971)
* present working sample

Through Eq. (4) we can account in our calibration also Fe53 transforming Eqs. (1)–(3). As displayed in Fig. 5, a good fit is achieved with a standard deviation $\sigma(O-C) = \pm 0.52$ Å.

A relevant issue when using Fe52 and Fe53 as indicators of absolute metallicity in the galaxies, is the fact that in this case we are possibly dealing with stellar populations of super-solar metallicity. This might be a problem in principle as there is no general consensus about the absolute calibration of super metal-rich stars in the Galaxy, and still large discrepancies persist among the different authors. It is important therefore to assess the problem in some detail in order to estimate the uncertainty affecting our inferred metallicity scale at large [Fe/H].

Four supplementary reference sources for stellar metal-

© American Astronomical Society • Provided by the NASA Astrophysics Data System

1994AJ....107..513B

TABLE 3. Supplementary metallicity scales.

Reference	number of stars	[Fe/H] Δ	[Fe/H] σ	Fe52 $\overline{(O-C)}$	Fe52 σ	Fe53 $\overline{(O-C)}$	Fe53 σ
Cayrel de Strobel et al. (1985)	36	—	—	0.05	0.70	0.19	0.89
Cayrel de Strobel et al. (1992)	34	0.01	0.08	−0.04	0.54	0.07	0.69
Gorgas et al. (1993)	22	0.01	0.13	−0.03	0.62	0.13	0.83
Taylor (1991)	13	−0.07	0.16	−0.19	0.37	−0.16	0.50
Hansen and Kjaergaard (1971)	13	−0.21	0.26	−0.02	0.61	0.12	1.00

licity have been accounted for in addition to Cayrel de Strobel *et al.* (1985), i.e., Hansen & Kjaergaard (1971) based on narrow-band photometry of Dickow *et al.* (1970), Taylor (1991), the recent upgraded version of the catalogue of Cayrel de Strobel *et al.* (1992), and Gorgas *et al.* (1993) for their stars in the sample. A total of 36 fiducial super metal-rich stars have been selected from our observations and from Faber *et al.* (1985) and Gorgas *et al.* (1993), and are listed in Table 2. To be included in the table stars should have reported a metallicity [Fe/H] $\geqslant$0.10 in at least one of the previous sources.

Taking as reference Cayrel de Strobel *et al.* (1985), we computed in Table 3 the mean offset Δ[Fe/H] and mean Fe52 and Fe53 residuals for the stars having supplementary metallicity determinations from the other sources. A certain shift among the different metallicity scales can be noticed. In particular, while a substantial agreement exists between Cayrel de Strobel *et al.* (1985, 1992) and Gorgas *et al.* (1993), on the contrary Taylor (1991) and especially Hansen & Kjaergaard (1971) tend to attribute a lower [Fe/H]. The results are plotted in Fig. 6, while in Fig. 7 we display the global distribution of the data according to the different metallicity scales. Quite comfortingly, it is fair to see that within the observational uncertainties no evident drifts are observed in the data, thus giving confidence that our adopted calibration still holds also for super metal-rich stellar populations.

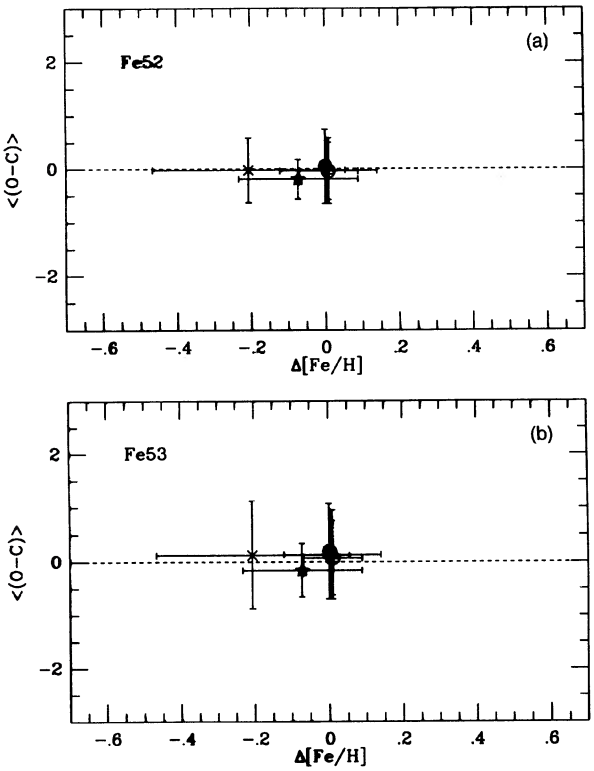

FIG. 6. (a),(b) Mean metallicity offsets vs mean index residuals from Eqs. (1) to (3) for the whole sample of 36 super metal-rich stars collected from present work, Faber *et al.* (1985), and Gorgas *et al.* (1993). The Δ[Fe/H] is computed with respect to the metallicity scale in Cayrel de Strobel *et al.* (1985) (● marker). Supplementary metallicity determinations are from Cayrel de Strobel *et al.* (1992) (○), Gorgas *et al.* (1993) (△), Taylor (1991) (*), and Hansen & Kjaergaard (1971) (×).

2.2 The Hβ Index

The Balmer lines, and in particular Hβ, are of strategic importance in the study of integrated spectra of stellar populations. The different stellar contributors act in fact in a quite composite way as the absorption feature basically traces the warm-star component while the local continuum is still strongly modulated by a 20%–40% contribution from stars in the red (RGB) and asymptotic giant branches (AGB) (Buzzoni 1989).

The resulting equivalent width of Hβ comes therefore from a balance of the different effects, and in general it can be regarded as an indicator of the relative weight in terms of *B*-luminosity contribution from the upper stellar MS with respect to the rest of the population. The obvious consequence is therefore that Hβ could be an effective indicator of the turn off temperature of a stellar population.

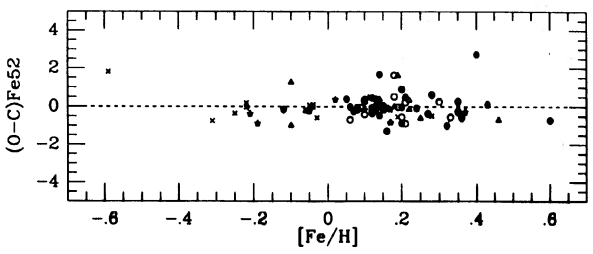

FIG. 7. Residuals of Fe52 from fitting Eqs. (1) to (3) vs [Fe/H] for the sample of 36 super metal-rich stars of Table 2 according to different metallicity scales from Cayrel de Strobel *et al.* (1985, 1992), Gorgas *et al.* (1993), Taylor (1991), and Hansen & Kjaergaard (1971). Point markers as in Fig. 6.

© American Astronomical Society • Provided by the NASA Astrophysics Data System

1994AJ....107..513B

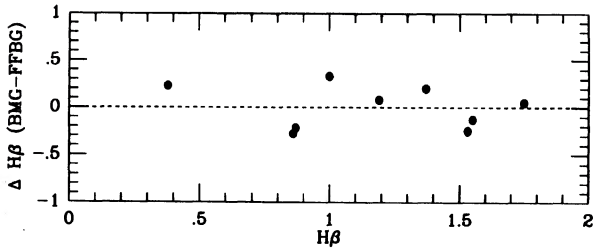

FIG. 8. Calibration residuals of Hβ for the nine standard stars in common with Faber *et al.* (1985). The standard system is reproduced within $\sigma_{H\beta} = \pm 0.23$ Å.

Calibration of the Hβ index in our data proceeded in a fully similar way to that for the iron indices. The index is defined as a pseudoequivalent width of the feature in the window (4849.50–4877.00)Å with respect to a local continuum interpolated between two side windows at (4829.50–4848.25)Å and (4878.25–4892.00)Å. The same primary standards from Faber *et al.* (1985) as for Fe52 provided the relation of transformation to be applied to the instrumental indices. The instrumental system proved to be nearly identical to the standard, and only a 0.10 Å offset was needed to be added to our observations. After this little correction, the standard system was matched within a ±0.23 Å accuracy (see Fig. 8), and also for this index adopted values for stars are reported In Table 1. Like for the iron indices, also for Hβ we did not correct for rotational line broadening as in any case it would be a negligible effect. Following the same procedure as for Fe52 and Fe53, photon statistics were found to be the main source of internal error in the index providing a typical internal error of ±0.13 Å.

The relationship between Hβ, Fe52, and Mg_2 (taken from Paper I) for our working sample is reported in the first two panels of Fig. 9. while in the third panel we display its dependence on temperature. It is fair to note that our data fully agrees with Gorgas *et al.*'s (1993) observations (once their $V-K$ is translated to temperature, e.g., via Johnson 1966). It appears that the line strength correlates negatively with temperature, and this fact can pose a supplementary constraint when studying the unresolved cm diagram of a SSP as on the contrary, the other indices move in the opposite sense.

In order to assure a more suitable coverage of the temperature range spanned by the stellar populations of globular clusters [with extended blue horizontal branches (HBs)], our observational stellar sample would also need to include stars at higher temperatures. However, in this case theoretical model atmospheres can effectively help as there are no substantial problems for current models in reproducing the Balmer lines. In particular, Kurucz (1979) supplied very accurate Hβ line profiles from which we easily derived the theoretical index for stars up to 20 000 K.

It is remarkable to note that due to the way the Hβ index has been defined, its value largely underestimates the real equivalent line width for stars warmer than 6500 K.

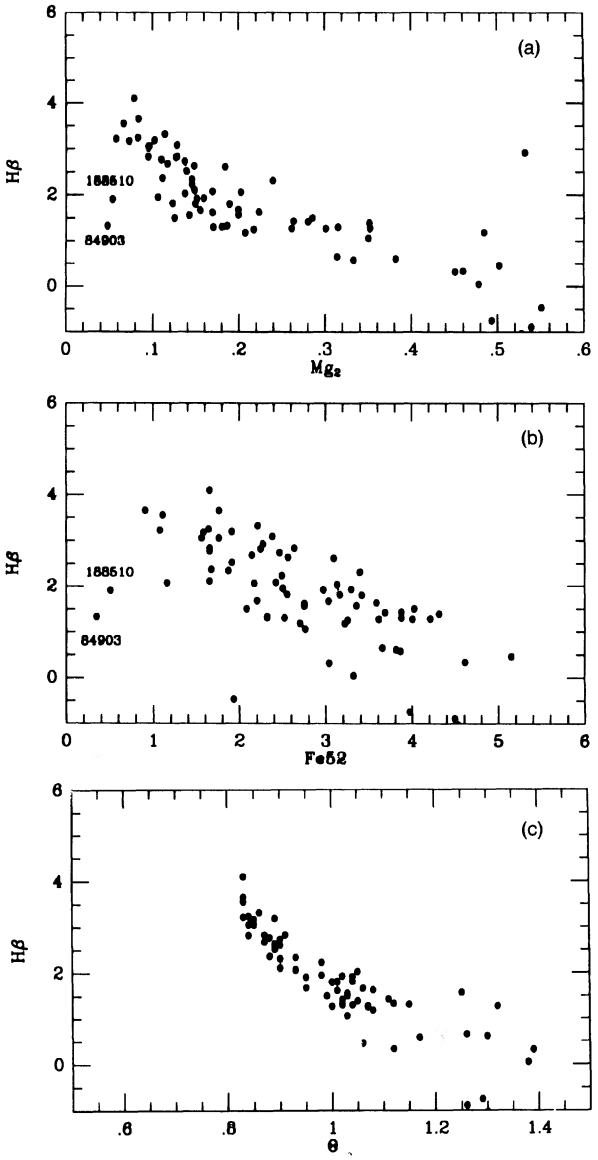

FIG. 9. (a)–(c) Relationship between Hβ index and magnesium, iron, and temperature in the stellar working sample. In panels a and b the two deviating points for metal-poor stars are labeled. Note also the large scatter among red dwarfs for $Mg_2 \geqslant 0.45$ with Hβ both in absorption and emission.

The reason is that the index window is only 27.5 Å wide, and the Stark-broadened wings of the line in hot stars overflows. This induces two combined effects that work decreasing the effective line strength. From one side we loose the wings of the line, and from the other side they affect the side windows decreasing the pseudocontinuum. This is shown in Fig. 10 where equivalent widths of Hβ are displayed along with the inferred photometric index. One can see that a reduction up to 50% is necessary at about 10 000 K (see also Worthey 1992). However, it is fair to note that the index smoothly matches our observations at cooler temperatures.

Resting on the extended model atmospheres and our

© American Astronomical Society • Provided by the NASA Astrophysics Data System

1994AJ....107..513B

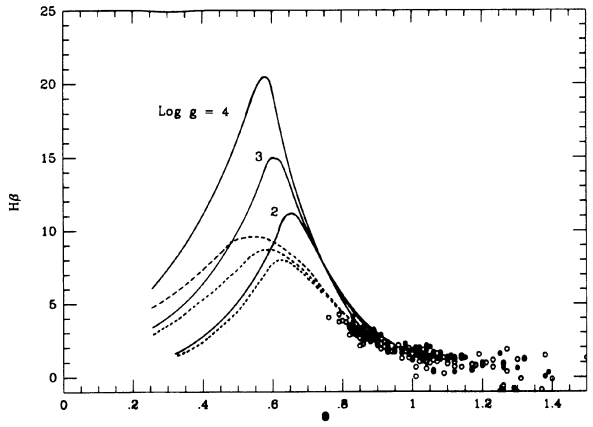

FIG. 10. Trend of Hβ index at higher temperatures. Solid lines display the equivalent width of the feature derived from the Kurucz (1979) model atmospheres for three values of stellar gravity, i.e., $\log g=4,3,2$. Dashed lines display on the contrary the pseudoequivalent widths for the same gravities according to Faber *et al.*'s (1985) definition of the index. The large difference is due to the overflow of the Stark broadened wings in the feature at hot temperatures. Stars in our working sample and in the Faber *et al.* (1985) and Gorgas *et al.* (1993) samples are displayed for reference as full and open dots, respectively.

observational database we attempted a fit of the index over the whole range in temperature. At high temperature we obtain

$$\log \mathrm{H}\beta=\frac{4.93}{\log g}\Theta-\frac{3.92}{\log g}+1.35. \quad (5)$$

The index reaches then a maximum at

$$\log \mathrm{H}\beta_{\mathrm{MAX}}=0.05\log g+0.80. \quad (6)$$

and decreases in cool stars following

$$\log \mathrm{H}\beta=-\left(\frac{1.28}{6.3-\log g}+1.4\right)\Theta+\frac{0.794}{6.3-\log g}+1.82. \quad (7)$$

The suitable range pertinent to each equation is derived assuming $\log \mathrm{H}\beta=\inf$ [Eqs. (5)–(7)]. Also for this index we show in Fig. 11 the residual distribution of the fit. Disregarding red dwarfs with $\Theta\geqslant 1.4$ for which Hβ is very weak and displays a large intrinsic scatter often being in emission, we obtain $\sigma(O-C)=\pm 0.34$ Å for 68 stars in our working sample, and $\sigma(O-C)=\pm 0.36$ Å including also stars in the Faber *et al.* (1985) and Gorgas *et al.* (1993) samples for a total of 191 objects.

3. SYNTHETIC MODELS

Star fitting functions previously derived provided the basic reference relations for synthesizing indices in stellar population models. The wide set of models for SSPs of Paper I, based on Buzzoni's (1989) code for population synthesis were accounted for, supplying here synthetic Fe52, Fe53, and Hβ in addition to Mg_2. The results are summarized in the series of Tables 4 to 6 exploring three different initial mass functions (IMFs) in the canonical form of a power law with varying the exponent s (the Salpeter IMF is referred to in our models with $s=2.35$).

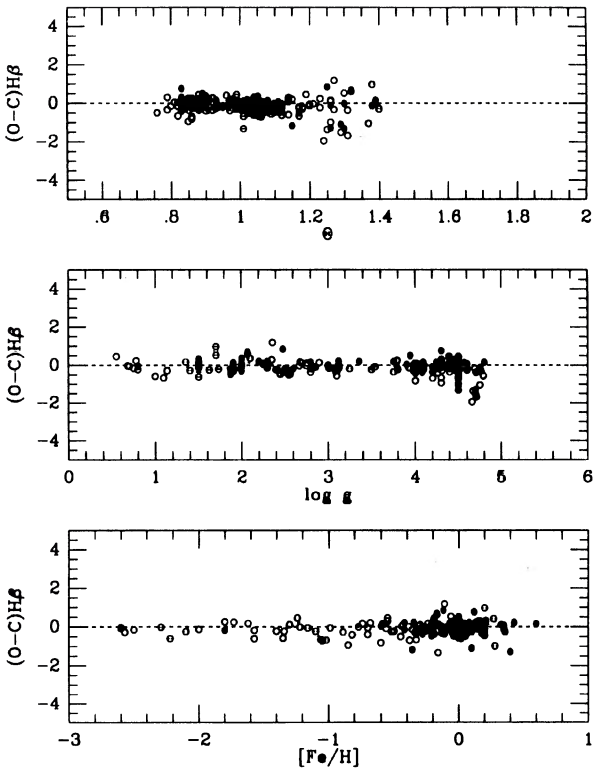

FIG. 11. Residuals of Hβ from adopted calibration [Eqs. (5) to (7)]. Points have the same meaning as in Fig. 3, with no systematic drift respect to temperature, gravity, and metallicity. Considering only the 68 stars in our working sample warmer than 3600 K (i.e., $\Theta\leqslant 1.4$) the scatter is ±0.34 Å while including also the Faber *et al.* (1985) and Gorgas *et al.* (1993) samples we have a total of 191 stars with a scatter of ±0.36 Å.

In each table indices are displayed with increasing metallicity, and for ages between 4 and 18 Gyr. A different stellar mass loss efficiency has been accounted for via the Reimers coefficient η (cf. Buzzoni 1989) selected in the range 0.3–0.5 according to what is inferred for globular clusters in the Galaxy and in the Magellanic Clouds (Fusi Pecci & Renzini 1978; Reid & Mould 1985).

In the tables, integrated indices for iron and Hβ are given as pseudoequivalent widths in Å. Operationally, they were calculated starting from the fitting functions in the previous section defining the indices in the single stars of a SSP. Suppose the window including the spectral feature have a width Δ (namely 38.75 Å for F52 and F53, and 27.50 Å for Hβ). For one star we have

$$F'_f=\frac{F_f}{F_c}=\frac{\Delta-I}{\Delta}, \quad (8)$$

where I is the value of the index, and $F'_f=F_f/F_c$ is the mean flux density in the window relative to the level of the local continuum interpolated from the two sidebands. Summing up over the whole stellar population we have

$$I_{\mathrm{TOT}}=\Delta\left[1-\frac{\Sigma(F'_fF_c)_j}{\Sigma(F_c)_j}\right]. \quad (9)$$

© American Astronomical Society • Provided by the NASA Astrophysics Data System

1994AJ....107..513B

TABLE 4. SSP models for $s=1.35$.

			$\eta = 0.3$			$\eta = 0.5$		
Log Z	[Fe/H]	Age (Gyr)	*Fe*52	*Fe*53	$H\beta$	*Fe*52	*Fe*53	$H\beta$
−4.00	−2.27	8.0	0.05	0.03	3.81	0.05	0.03	3.89
		10.0	0.09	0.05	3.07	0.08	0.05	3.12
		12.5	0.27	0.15	2.75	0.24	0.13	2.79
		15.0	0.33	0.18	2.57	0.30	0.16	2.60
		18.0	0.39	0.22	2.40	0.35	0.19	2.44
−3.00	−1.27	8.0	1.17	0.80	2.78	1.16	0.79	2.82
		10.0	1.21	0.82	2.56	1.20	0.82	2.59
		12.5	1.26	0.86	2.37	1.25	0.85	2.41
		15.0	1.32	0.90	2.24	1.30	0.89	2.27
		18.0	1.38	0.94	2.11	1.36	0.92	2.16
−2.00	−0.25	4.0	1.91	1.42	2.69	1.92	1.43	2.71
		5.0	2.07	1.55	2.48	2.08	1.56	2.50
		6.0	2.16	1.62	2.35	2.17	1.63	2.37
		8.0	2.32	1.76	2.15	2.34	1.77	2.17
		10.0	2.43	1.86	2.02	2.45	1.87	2.03
		12.5	2.56	1.97	1.88	2.58	1.99	1.89
		15.0	2.62	2.03	1.79	2.64	2.05	1.81
−1.77	−0.02	4.0	2.29	1.74	2.48	2.30	1.76	2.49
		5.0	2.40	1.84	2.33	2.42	1.86	2.35
		6.0	2.50	1.93	2.22	2.52	1.95	2.23
		8.0	2.67	2.09	2.03	2.69	2.11	2.04
		10.0	2.81	2.23	1.88	2.83	2.25	1.89
		12.5	2.92	2.34	1.75	2.94	2.36	1.77
		15.0	3.00	2.42	1.66	3.02	2.44	1.67
−1.54	0.22	4.0	2.69	2.13	2.30	2.71	2.14	2.31
		5.0	2.79	2.22	2.19	2.80	2.24	2.20
		6.0	2.90	2.33	2.07	2.91	2.34	2.08
		8.0	3.07	2.51	1.89	3.09	2.52	1.90
		10.0	3.21	2.66	1.75	3.23	2.67	1.76
		12.5	3.33	2.78	1.63	3.35	2.80	1.64
		15.0	3.42	2.88	1.54	3.44	2.90	1.55

As pointed out by Faber *et al.* (1985), both Fe and $H\beta$ indices can no longer be regarded as true equivalent widths as the feature window and the continuum sidebands often include also spurious blends (e.g., the iron line at 5335 Åaffects the continuum window for calculating Mg_2, while the red sideband of $H\beta$ and the feature itself are affected by other Fe blends below 6000 K). Moreover, in the case of $H\beta$ we have to properly account for the fact the feature strength in hot stars is decreased with most of the line wings lost in the side pseudocontinuum windows.

An illuminating example of the way stars in the different branches of the cm diagram contribute to the integrated index of the SSP is displayed in Figs. 12 and 13 both for Fe52 and for $H\beta$. A Salpeter 15 Gyr population of solar metallicity and with a red HB (RHB in the Buzzoni 1989 notation) is assumed. One can see that while the iron index is mainly provided by stars at the base of the RGB, integrated $H\beta$ mainly comes from stars in the upper MS about the turnoff point. Also in case we introduce a bluer HB, while it will certainly affect the feature, in no way it can become the major contributor to $H\beta$. Single HB stars are in fact more luminous than the turnoff stars but the latter ones are always much more numerous.

4. METALS IN EARLY TYPE GALAXIES AND GLOBULAR CLUSTERS

On the basis of the fitting functions previously derived, and coupling with the Mg_2 discussion of Paper I, we are now in the position of approaching more quantitatively some basic questions dealing with the chemical evolution in early type galaxies and globular clusters. It is useful to carry on our analysis comparatively as to some extent stellar populations in globular clusters can be regarded as a natural extension to metal-poor regimes of the stellar populations in the elliptical galaxies (Frogel *et al.* 1980; Burstein *et al.* (1984); Paper I).

A first important application of theoretical calculations is a comparison of the metallicity scale of SSPs inferred from Fe52 and $H\beta$ with the current metallicity scale for

© American Astronomical Society • Provided by the NASA Astrophysics Data System

1994AJ....107..513B

TABLE 5. SSP models for $s=2.35$.

			$\eta = 0.3$			$\eta = 0.5$		
Log Z	[Fe/H]	Age (Gyr)	*Fe*52	*Fe*53	*Hβ*	*Fe*52	*Fe*53	*Hβ*
−4.00	−2.27	8.0	0.10	0.07	3.73	0.11	0.07	3.79
		10.0	0.16	0.10	3.00	0.15	0.10	3.04
		12.5	0.34	0.20	2.66	0.32	0.18	2.70
		15.0	0.40	0.23	2.48	0.38	0.22	2.51
		18.0	0.46	0.27	2.32	0.43	0.25	2.35
−3.00	−1.27	8.0	1.18	0.81	2.75	1.17	0.80	2.78
		10.0	1.23	0.84	2.52	1.22	0.84	2.56
		12.5	1.29	0.88	2.33	1.28	0.88	2.36
		15.0	1.35	0.92	2.19	1.34	0.92	2.22
		18.0	1.41	0.97	2.06	1.39	0.95	2.10
−2.00	−0.25	4.0	1.91	1.43	2.69	1.92	1.43	2.71
		5.0	2.07	1.55	2.48	2.08	1.56	2.50
		6.0	2.18	1.64	2.34	2.19	1.65	2.36
		8.0	2.34	1.78	2.14	2.36	1.79	2.15
		10.0	2.46	1.88	1.99	2.47	1.90	2.01
		12.5	2.58	2.00	1.85	2.60	2.01	1.86
		15.0	2.65	2.06	1.75	2.67	2.08	1.77
−1.77	−0.02	4.0	2.30	1.76	2.48	2.31	1.77	2.49
		5.0	2.42	1.86	2.32	2.43	1.88	2.34
		6.0	2.52	1.96	2.20	2.54	1.97	2.22
		8.0	2.69	2.12	2.00	2.71	2.14	2.02
		10.0	2.84	2.26	1.85	2.85	2.27	1.86
		12.5	2.95	2.37	1.72	2.97	2.39	1.73
		15.0	3.03	2.45	1.62	3.05	2.47	1.63
−1.54	0.22	4.0	2.71	2.15	2.29	2.73	2.16	2.30
		5.0	2.82	2.25	2.18	2.83	2.27	2.19
		6.0	2.93	2.36	2.06	2.94	2.38	2.07
		8.0	3.10	2.54	1.87	3.12	2.56	1.87
		10.0	3.24	2.69	1.72	3.26	2.70	1.73
		12.5	3.36	2.81	1.59	3.38	2.83	1.60
		15.0	3.45	2.91	1.49	3.47	2.92	1.50

Galactic and M31 globular clusters. A tentative calibration is shown in the two panels of Fig. 14 facing cluster observations from Burstein *et al.* (1984). The adopted cluster metallicity scale is that of Zinn & West (1984) extended by Brodie & Huchra (1990) to M31 clusters via IR observations by Aaronson *et al.* (1978), and Frogel *et al.* (1980). In the figure we do not consider Fe53 but it would be immediate to account for it starting also from Fe52 since the two indices are strictly dependent.

4.1 Oxygen Enhancement in Globular Clusters

The basic reference models originating the solid line calibrations in Fig. 14 assume 15 Gyr SSPs with $s=2.35$ and a RHB morphology. According to our previous discussion, treatment of AGB in the models has been such as its extension was cut in luminosity at the level of the RGB through an appropriate choice of the parameter η modulating stellar mass loss. This assumption would not have, however, any important effect on Fe52 (and even less on Hβ) since in any case stars at the base of the RGB still remain the main contributors to the integrated index.

A change in the HB morphology adopting a bluer IHB (in the Buzzoni 1989 notation) observed in metal-poor globulars is also accounted for in the two panels of the figure (dashed lines). As expected, Fe52 is negligibly affected by this change while a more important variation is induced for Hβ which systematically raises in excess of 0.7 Å. Although the differential change is in agreement with the empirical estimate by Burstein *et al.* (1984, see their Fig. 5k), it is in the sense of strongly worsen the match to the data, and both Galactic and M31 globulars lie now well below the fiducial line.

Also acting on IMF we would not substantially improve the fit. A check on Tables 4–6 makes evident that one should not expect any relevant change both in Fe52 and Hβ. Although with a different behavior, both indices are scarcely sensitive to the cool stars at the extreme limits of mass, i.e., giants at the tip of AGB and dwarfs at the faint end of the MS (remember that Fe52 fades cooler than 4000

© American Astronomical Society • Provided by the NASA Astrophysics Data System

1994AJ....107..513B

TABLE 6. SSP models for $s=3.35$.

			$\eta = 0.3$			$\eta = 0.5$		
Log Z	[Fe/H]	Age (Gyr)	*Fe52*	*Fe53*	*Hβ*	*Fe52*	*Fe53*	*Hβ*
−4.00	−2.27	8.0	0.23	0.15	3.49	0.24	0.16	3.54
		10.0	0.31	0.20	2.77	0.31	0.20	2.80
		12.5	0.49	0.29	2.44	0.47	0.29	2.47
		15.0	0.54	0.33	2.27	0.53	0.32	2.29
		18.0	0.60	0.36	2.11	0.58	0.35	2.14
−3.00	−1.27	8.0	1.23	0.85	2.60	1.23	0.85	2.63
		10.0	1.28	0.88	2.40	1.27	0.88	2.42
		12.5	1.35	0.93	2.20	1.34	0.93	2.22
		15.0	1.41	0.97	2.06	1.40	0.97	2.08
		18.0	1.47	1.01	1.93	1.46	1.00	1.96
−2.00	−0.25	4.0	1.94	1.45	2.64	1.95	1.46	2.65
		5.0	2.11	1.58	2.42	2.11	1.59	2.43
		6.0	2.21	1.67	2.28	2.22	1.68	2.29
		8.0	2.37	1.81	2.06	2.38	1.82	2.07
		10.0	2.49	1.91	1.91	2.50	1.92	1.92
		12.5	2.60	2.02	1.75	2.62	2.03	1.77
		15.0	2.67	2.08	1.66	2.68	2.09	1.67
−1.77	−0.02	4.0	2.33	1.79	2.41	2.34	1.80	2.42
		5.0	2.45	1.89	2.24	2.46	1.91	2.26
		6.0	2.55	1.99	2.12	2.57	2.00	2.14
		8.0	2.72	2.14	1.92	2.73	2.16	1.93
		10.0	2.84	2.27	1.75	2.86	2.28	1.76
		12.5	2.94	2.37	1.61	2.96	2.38	1.62
		15.0	3.01	2.43	1.51	3.02	2.45	1.52
−1.54	0.22	4.0	2.75	2.19	2.23	2.76	2.20	2.24
		5.0	2.85	2.29	2.11	2.86	2.30	2.12
		6.0	2.95	2.39	1.98	2.97	2.41	1.99
		8.0	3.12	2.56	1.78	3.13	2.57	1.79
		10.0	3.25	2.69	1.63	3.26	2.71	1.64
		12.5	3.34	2.80	1.49	3.36	2.81	1.50
		15.0	3.42	2.88	1.39	3.43	2.89	1.40

K and Hβ is negatively correlated with temperature). We would not take advantage therefore of a larger baseline in stellar mass within the population, with a consequent weak response to a change in the IMF. Incidentally, things can be different for Mg_2, as shown in Paper I, since it always keeps to increase with decreasing temperature.

The apparent discrepancy in the hydrogen index seems to decidedly point to a relevant change in our adopted evolutionary scenario for globular clusters. Two ways out can be realistically envisaged to recover the question. As shown in previous section, Hβ is basically an indicator of temperature of the upper MS, and in particular of the turn-off point. As a consequence, if we want to decrease synthetic values in the SSPs without any change in the iron indices (and in Mg_2 as well) we should move the upper MS to lower temperatures (and hopefully also decrease its luminosity). This is equivalent to increased age in the isochrones and/or consider the case of enhanced CNO elements.

A revised set of O-enhanced isochrones in the suitable range for fitting globular cluster cm diagrams has been

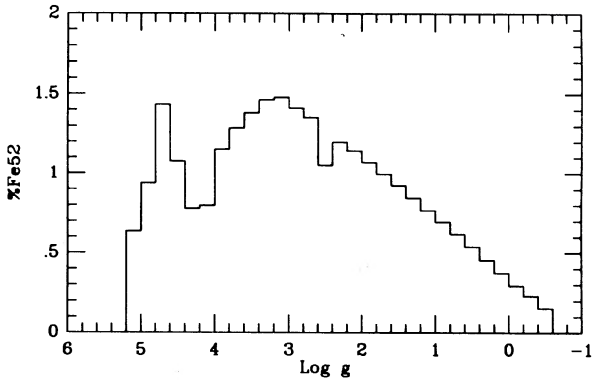

FIG. 12. Disaggregated contributions to the Fe52 feature from stars of different gravity in a 15 Gyr Salpeter SSP with solar metallicity and RHB morphology. The quantity displayed is the ratio of the relative contribution of each stellar bin to the continuum and to the residual light in the absorption feature. A value about 1.0 indicates that stars contribute with the same weight both to continuum and to the line, while values in excess of unity means that those stars mainly contribute to the absorption feature. It is immediate to see that integrated Fe52 is mainly contributed by stars at the base of the RGB about $\log g \sim 3.0$.

© American Astronomical Society • Provided by the NASA Astrophysics Data System

1994AJ....107..513B

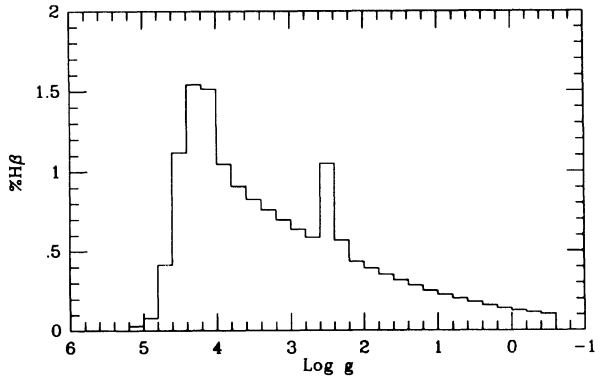

FIG. 13. Same as in Fig. 12 but for Hβ. One sees that the index better responds to stars in the upper MS about $\log g \sim 4.1$. The bump in the histogram about $\log g \sim 2.3$ is due to the assumed RHB.

recently published by Bergbush & VandenBerg (1992) based on VandenBerg's (1992) new evolutionary tracks. Oxygen to iron excess is assumed to vary with changing metallicity following the well-established empirical relations $[O/Fe] = -0.5[Fe/H]$ for $[Fe/H] \geqslant -1$, and $[O/Fe] = -0.2[Fe/H] + 0.3$ for lower metallicities. For fixed age and global metallicity, post-MS evolution in O-enhanced isochrones does not substantially differ from the case of $[O/Fe] = 0$. On the contrary, the MS changes with the turnoff point becoming slightly cooler and less luminous by $\Delta \log T \sim 0.01$ and $\Delta \log L \sim 0.1$, respectively. The fit to cm diagrams of template globular clusters with the O-enhanced isochrones led Bergbush & VandenBerg (1992) to predict lower ages (about 14–15 Gyr) with respect to previous estimates relying on standard isochrones rather than indicating 18–19 Gyr (Buonanno *et al.* 1989).

Similar quantitative results are confirmed by Chieffi *et al.* (1991), and Straniero *et al.* (1992), who extensively discussed the case of isochrones with nonstandard chemical mixtures. As briefly summarized also in Paper I, any selective variation in the CNO chain would act mainly on the MS by changing the nuclear clock of the stars. On the contrary, the location of the RGB would not be affected, rather responding to a change in the relative abundance of the heavy α elements like Mg, Si, Fe that are important e^- donors thanks to their lower potential of ionization and are therefore the main contributors to the atmospheric opacity in the giant stars (Renzini 1977).

A simple but effective procedure to account for Bergbush & VandenBerg's (1992) results has been attempted by slightly modifying the VandenBerg (1983) standard isochrones with $[O/Fe] = 0$, originally used in the Buzzoni (1989) code for synthesizing metal-poor populations. One can rather realistically mimic the effects of enhancing oxygen in the cm diagrams of a SSP by smoothly decreasing temperature and luminosity along the MS and subgiant branch (SGB) such as $\log T_{new} = \log T_{old} - \Delta \log T$ and $\log L_{new} = \log L_{old} - \Delta \log L$, where $\Delta \log T = 0.1(\log T_{old} - 3.7)$, with the supplementary boundary condition $\Delta \log T = 0$ in case it would become negative, while

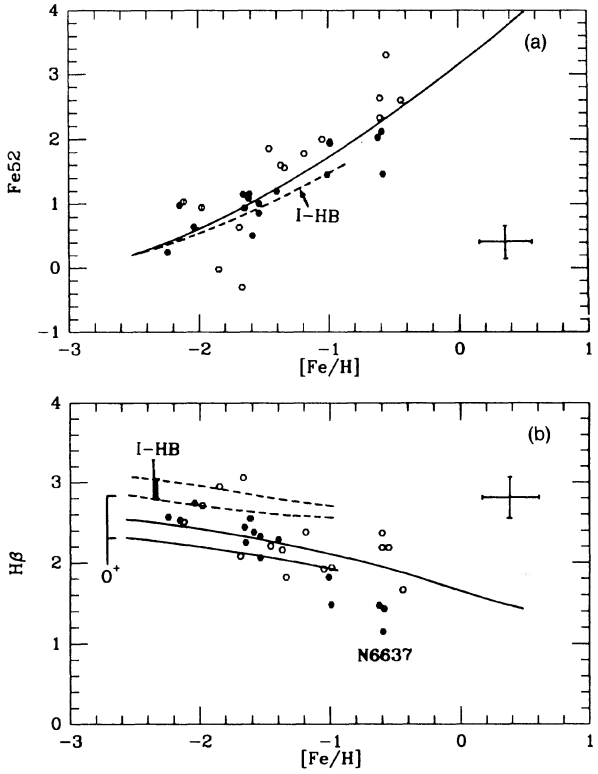

FIG. 14. (a),(b) Adopted calibration of Fe52 and Hβ indices vs [Fe/H]. Full and open dots represent Galactic and M31 globular clusters, respectively. Data are from Burstein *et al.* (1984) while metallicity scale is from Brodie & Huchra (1990). Typical error bars for the observations are also displayed. Solid lines are model sequences for 15 Gyr Salpeter SSPs with RHB morphology and standard metal mix (i.e., $[CNO/Fe] = 0$). Dashed lines display the change adopting an IHB. In panel b the effect of adopting O-enhanced isochrones for metal-poor populations is explored (labeled O^+). Both IHB and RHB sequences are decreased by about 0.3 Å allowing a better match to the data. The extreme discrepant case of NGC 6637 (M69) is also marked (see the text for discussion).

$\Delta \log L = 10\Delta \log T$ (see Fig. 1 in Chieffi *et al.* 1991 for a clarifying example).

The change in the expected Hβ calibration with these new improvements is added in Fig. 14 (for the reasons previously discussed no changes are induced on the contrary for Fe52). One sees that the Hβ strip constrained by IHB and RHB models is now decreased by about 0.3 Å, and meets much better observations. A similar trend would have obtained increasing age with standard isochrones, but ages no less than 18–20 Gyr were permitted in this case.

Between the two alternatives, we are inclined to believe that the O-enhanced case is more likely to be preferred as it is in the sense supported by observations of metal-poor Galactic field stars widely indicating a decoupling of O and Fe at low metallicity (see Gratton 1992 for a full discussion and review of this subject).

Despite the overall agreement in the new calibration, still some points for Galactic globulars clearly deviate in the figure also respect to homologue M31 clusters, the most notable case being that of NGC 6637 (M69). This fact led Burstein *et al.* (1984) to claim for a substantial

© American Astronomical Society • Provided by the NASA Astrophysics Data System

1994AJ....107..513B

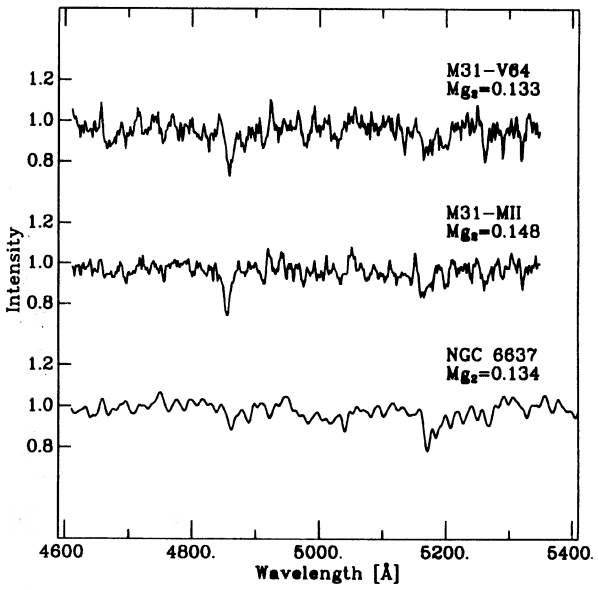

FIG. 15. Comparison between the spectrum of the Galactic globular cluster NGC 6637 (M69) and two clusters in M31 with similar metallicity inferred through the Mg_2 index. It is evident the strong Hβ deficiency in the Galactic cluster, possibly indicating an exceedingly low temperature of the turnoff region in the stellar population of the cluster. Observations of NGC 6637 come from our observational run (see Paper I for details), and spectrum has been degraded to a resolution of 10 Å in order to compare consistently with M31 clusters. Data for M31-V64 and M31-MII are unpublished observations of Battistini *et al.* (1987) taken at the Russian BTA-SAO 6 m telescope.

difference between the cluster stellar population in the Galaxy and in M31.

The spectrum of NGC 6637 taken during our second observing run (see Paper I for acquisition details) is compared in Fig. 15 with those of two M31 clusters with similar Mg_2 index (i.e., MII and V64) kindly made available to us by the Bologna group (Battistini *et al.* 1987). It is evident that this cluster displays an exceedingly low hydrogen feature respect to the M31 clusters apparently pointing to a super metal-rich population. More likely, this might be the most striking example of selective CNO enhancement as a fit to the cluster with standard isochrones would call for unrealistically old ages. The apparent discrepancy between globulars in the Galaxy and M31 might be witnessing therefore a different genesis in the enrichment of light α elements with the M31 population sharing a more standard chemical mix.

Turning back again to Fig. 14, a last crucial warning is that [Fe/H] in the models comes in fact from a translation of Z, i.e., the global metallicity of a population. Comparing with globular clusters therefore we tacitly accept that iron is there an unbiased tracer of the whole metallicity. The eventual calibration of Fe52, Fe53, and Hβ vs [Fe/H] as it stems from the standard (i.e., [CNO/Fe]=0) models for population synthesis is reported in Table 7.

4.2 Iron Content in Elliptical Galaxies

Previous discussion on globular clusters led to some firm conclusions that could address more confidently our analysis to elliptical galaxies. To summarize, essentially three leading points emerged.

First, the Fe indices are optimal indicators of genuine metallicity effects in SSPs. Both Fe52 and Fe53 weakly depend on the assumed IMF and age, and they are almost insensitive to any realistic HB evolution. Mass loss and details of AGB evolution are not crucial, and the indices basically report on the moderately cool stellar component about the base of the RGB. The main characteristics of the Fe indices is therefore a direct dependence on [Fe/H] not via temperature effects.

Second, Hβ reports on the status of the warm component in a population, with special attention to the temperature distribution of the turnoff and SGB region. It greatly increases in presence of a blue HB, and in any case a RHB morphology provides the lower envelope for the integrated index at any metallicity. Its dependence on metallicity is fully induced by the indirect effects on the temperature distribution of the upper MS.

TABLE 7. Adopted calibration vs [Fe/H].*

	s=1.35			s=2.35			s=3.35		
[Fe/H]	Fe52	Fe53	Hβ	Fe52	Fe53	Hβ	Fe52	Fe53	Hβ
−2.50	0.10	0.02	2.65	0.25	0.05	2.55	0.40	0.20	2.30
	(0.10)	(0.02)	(3.20)	(0.25)	(0.05)	(3.05)	(0.40)	(0.20)	(2.70)
−2.00	0.50	0.25	2.50	0.60	0.35	2.40	0.75	0.45	2.25
	(0.49)	(0.23)	(3.05)	(0.55)	(0.30)	(2.95)	(0.70)	(0.40)	(2.65)
−1.50	1.05	0.70	2.35	1.10	0.70	2.30	1.20	0.80	2.15
	(0.95)	(0.60)	(2.85)	(0.95)	(0.60)	(2.80)	(1.05)	(0.70)	(2.60)
−1.00	1.65	1.20	2.20	1.70	1.20	2.10	1.75	1.20	2.00
	(1.45)	(1.05)	(2.70)	(1.45)	(1.05)	(2.70)	(1.55)	(1.10)	(2.50)
−0.50	2.30	1.75	1.95	2.35	1.80	1.90	2.40	1.80	1.80
0.00	3.05	2.50	1.65	3.10	2.55	1.65	3.10	2.50	1.55
0.25	3.45	2.90	1.50	3.50	2.90	1.50	3.45	2.90	1.35
0.50	3.85	3.40	1.45	3.95	3.30	1.45	3.85	3.30	1.35

*Entries in parentheses refer to an I–HB morphology.

© American Astronomical Society • Provided by the NASA Astrophysics Data System

1994AJ....107..513B

A third remark that could be worth adding from Paper I is that Mg_2 complements the analysis reporting on the contrary on the distribution of the cooler stars in a SSP along the AGB and RGB, and at the faint tail of the MS. As shown in Paper I, Mg_2 is a metallicity indicator essentially due to its dependence on the location of the giant branches.

Thanks to the different behaviors, the three indices respond selectively to a change in the chemical mixture. To summarize, a variation in the light α elements (namely the CNO chain) modifies the shape of the turnoff region, and in case it is better tracked by $H\beta$; a nonstandard partition of the Mg, Si, Fe group affects on the contrary the location of the RGB via a change in the atmosphere opacity, and it mainly acts on Mg_2. Finally, the Fe indices allow an independent and important check on iron trend with respect to the global metallicity of SSPs.

The overall observed distribution of early type galaxies and globular clusters in the Fe52/Mg_2 and $H\beta$/Mg_2 planes is reported in the two panels of Fig. 16. In addition to previous observations of Galactic and M31 globulars we display data for ellipticals from Worthey *et al.* (1992), and from Gorgas *et al.* (1990). Both sources assured a fully consistent set of observations for galaxies, with similar procedures for data treatment.

We reported in the figure the locus of our fiducial calibration for 15 Gyr SSPs with Salpeter IMF and RHB (solid line). The supplementary correction to $H\beta$ for O-enhanced globular cluster populations is also replied in the lower panel both for the RHB and IHB cases.

Two striking features stem from the analysis of the figure. In the Fe52/Mg_2 plot it is quite evident that while the bulk of galaxy distribution is completely matched by models about solar metallicity, observations display a fully different slope with respect to theoretical expectations in the sense of a weaker dependence on Mg_2.

In a preliminary attempt to account for such different trend, Worthey *et al.* (1992) compared data with a selected set of original models for 18 Gyr SSPs edging along the upper envelope of the observations (see their Fig. 2). This led them to conclude that a systematic magnesium overabundance or iron deficiency would be implied by the data. The authors correctly stressed the potential relevance of such a discrepancy discussing a number of possible astrophysical implications. In particular, they pointed out that the Fe deficiency might be witnessing a somehow general deficiency in SNe I feeding heavy elements in elliptical galaxies respect for instance to spirals.

There is a widespread consensus about the role of supernovae in the metal enrichment of galaxies (see, e.g., Trimble 1991 for a recent review), and especially the role of SNe I (possibly dealing with binary systems of low-mass stars) has been emphasized as a main channel for iron enrichment in ellipticals galaxies. Greggio & Renzini (1983a,b) and Matteucci & Greggio (1986) performed specific calculations in this regard showing that Fe enrichment via SN events should proceed in early type galaxies slowly over gigayears while light α elements should have

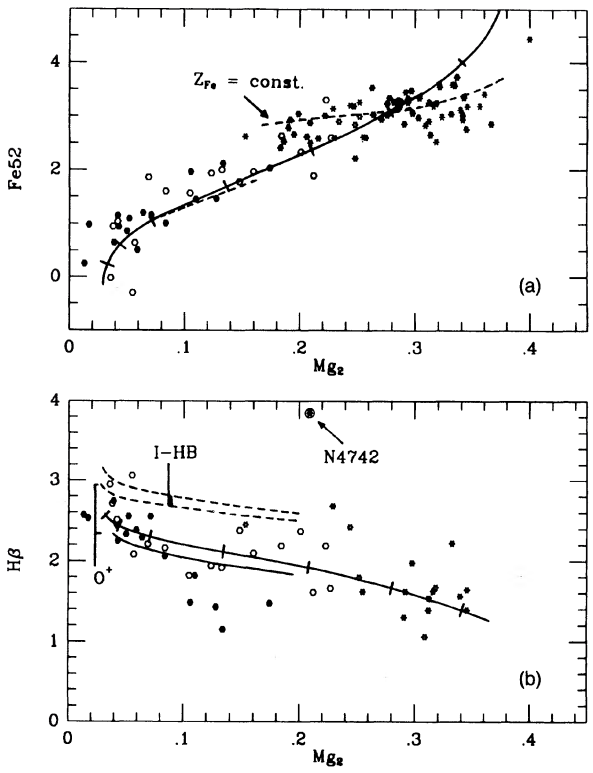

FIG. 16. (a),(b) Adopted metallicity calibration in the observational planes Fe52/Mg_2 and $H\beta$/Mg_2. Full and open dots are Galactic and M31 globular clusters from Burstein *et al.* (1984), while star and asterisk markers are for elliptical galaxies from Gorgas *et al.* (1990), and Worthey *et al.* (1992), respectively. Solid curves in both panels indicate the locus expected for standard 15 Gyr Salpeter SSP with RHB. Increasing values for [Fe/H] from -2.5 to $+0.5$ are marked along the curve every 0.5 dex in the sense of increasing Mg_2. The effect of adopting an IHB morphology at low metallicities (i.e., for $Mg_2 \geqslant 0.2$) is displayed in both panels by the dashed lines, while in panel b also the effect of O-enhanced models is accounted for (labels O^+). The Fe52 distribution for galaxies in panel a is better matched if the direct dependence of the index on stellar metallicity in the fitting functions [Eqs. (1)–(3)] is neglected (dashed curve about $Mg_2 \sim 0.28$). See the text for discussion.

been supplied to the galactic stellar populations in an extremely quicker way (Matteucci & Brocato 1990).

A slightly different scenario with respect to Worthey *et al.* (1992) is emerging from the present analysis of the data. Supporting the main conclusion in Paper I, we can confirm that the bulk of elliptical galaxy population has a global metallicity consistent or slightly more enhanced than solar. Both iron and magnesium appear to be in *average* in solar partition so that [Mg/Fe]$\rightarrow$0 when [Fe/H]$\rightarrow$0 but a trend does exist, and iron seems now apparently in excess in dwarf ellipticals and deficient in giant ellipticals.

The dashed line in the upper panel of Fig. 16 might give us the solution of the dilemma. It has been obtained by synthetic models resting on our previous fitting functions but this time we vanished the *direct* metallicity dependence of Fe52 in Eqs. (1)–(3). This is equivalent to saying that Z_{Fe} is constant throughout the model ellipticals, so that only the change in the isochrone location with varying Z is

© American Astronomical Society • Provided by the NASA Astrophysics Data System

1994AJ....107..513B

sufficient to fully account for the apparent trend of Fe52 with Mg_2. *Our main conclusion is therefore that the iron abundance per gram of matter in elliptical galaxies is constant.* If we assume iron to be fed by SNe I this is simply equivalent to state that the *integrated rate of SNe* I *per unit mass is at present constant among early type galaxies.*

It could be worth stressing that the apparent nonsense implied by the fact that Fe52 does not correlate with [Fe/H] completely relies on an ill-posed definition of metallicity for galaxies. In other words, what we would mean is that magnesium, and not iron is a rather more suitable tracer of the galactic global metallicity. Therefore, although it is unquestionable that Fe52 does depend on Z_{Fe} (via stellar [Fe/H]) in Eqs. (1)–(3), it can no longer depend on Z in ellipticals as Z_{Fe} is decoupled from Z.

A second important question that arises from Fig. 16 is that contrary to globular clusters, stellar populations in elliptical galaxies do not display any overabundance of CNO elements. The Hβ observations in the lower panel of the figure are in fact fairly well met by standard calibration supporting the canonical scenario relying on old metal-rich SSPs. The spread of galactic data might rather indicate the presence of a composite stellar population in elliptical galaxies in which the main bulk of metal-rich stars is slightly contaminated by Population II stars at low metallicity. There are signs that this contamination might be typically no more than 10%–15% of the total V light of a galaxy (Buzzoni 1993).

In order to fully reinforce our previous conclusions about Fe enrichment in elliptical galaxies we need to investigate, through a combined analysis of the galaxy distribution in both the Fe52/Mg_2 and Hβ/Mg_2 planes, also other alternative mechanisms able in principle to explain the trend in the data. In particular, we know that a spread in the galactic age could work in the right way.

With the help of the models in Paper I we have computed in Fig. 17 the expected evolutionary sequences for SSP of [Fe/H] = −0.5, 0.0, +0.5 evolving from 5 to 15 Gyr. As the sequences run nearly horizontally in the figure, a little uncertainty in the observed Fe52 would reflect in a large uncertainty the inferred age of a galaxy. However, it is clear that if this would be the case, galaxies should span an extremely large range of ages from less than 3 to 5 Gyr up to 15–20 Gyr or even more.

Supporting the arguments already discussed in Paper I, we are inclined to believe that, in this case, a spread in age among ellipticals could hardly be mainly responsible for the observed distribution of the galaxy population at present day. Following Paper I, the case of NGC 4742, for which we have extensive evidence for recent star formation (Burstein *et al.* 1988), could serve as an instructive example.

The galaxy is marked in Fig. 17 and it does not seem to display any peculiarity with respect to the rest of the population in the Fe52/Mg_2 plane. According also to Paper I we could assign to it an age about 5 Gyr or less assuming a solar or super solar metallicity, respectively. As far as the Hβ distribution is concerned [Fig. 16(b)], a clear discrepancy would appear. Here, NGC 4742 displays an exceedingly high value for Hβ, and lies well off the main clump of galaxies. This in reason of the fact that its recent star formation has strongly affected Hβ.

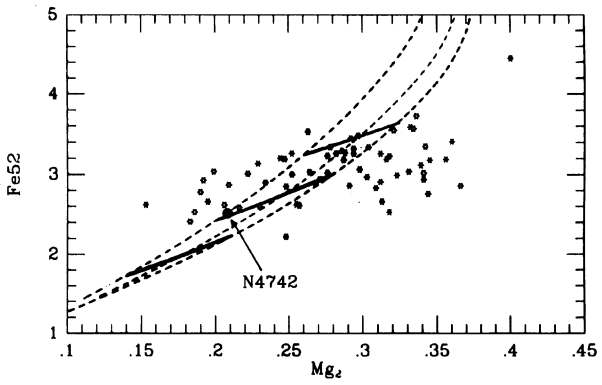

FIG. 17. Evolutionary sequences from 5 to 15 Gyr for three stellar populations with [Fe/H] = −0.5, 0.0, +0.5 (thick solid lines from bottom to top, respectively). Age increases in the sense of increasing Mg_2. Short-dashed curves are envelopes at 5, 10, and 15 Gyr with changing metallicity. Point markers as in Fig. 16. The galaxy NGC 4742 is singled out (see the text for discussion).

According to our previous discussion about the different sensitivity of the indices to age and metallicity effects, we should conclude therefore that the age of NGC 4742 is *not so usual* among present-day galaxies, that rather seem much older (and roughly coeval) objects.

The different behavior of the CNO and Fe trends between globulars and ellipticals basically supports a unified scenario in which metal enrichment driven by SNe was indirectly constrained by the total mass of the stellar systems via the galactic wind phase (Arimoto & Yoshii 1987; Arimoto 1988; Ferrini & Poggianti 1993). The low gravitational binding energy of globular clusters did not allow us to fully accomplish a complete chemical enrichment. Only primeval SNe II had time enough to supply light α elements while substantially no iron was produced at early stages (in a sense, rather than speaking of oxygen enhancement in globulars from the evolùtionary point of view we should speak of iron deficiency).

To complete the picture, elliptical galaxies with increasing mass retained with higher efficiency SN II ejecta (the total galactic binding energy is proportional to $M_{TOT}^{1.45}$; Saito 1979) increasing global metallicity, and moreover developed a higher fraction (proportional to M_{TOT}) of SN I supplying Fe. As galactic wind is inversely dependent on the galactic binding energy, light α elements from SN II enhanced in giant ellipticals respect to Fe, that was supplied on the contrary at a constant rate per unit mass.

5. CONCLUSIONS

In this work we addressed the problem of the chemical evolution in elliptical galaxies and globular clusters through a combined study of the iron indices Fe52 and Fe53, and of the Hβ line strength. The analysis further carries on previous results relying on the study of the magnesium Mg_2 index made in Paper I.

© American Astronomical Society • Provided by the NASA Astrophysics Data System

1994AJ....107..513B

Observations of a set of standard stars (both dwarfs and giants) allowed us to explore in great detail the dependence of the indices vs the physical stellar parameters, namely temperature, gravity, and metallicity. This converged into a set of fitting functions that were included into Buzzoni's (1989) code for population synthesis in order to derive expected integrated indices in stellar aggregates.

A wide set of SSPs has been computed deriving synthetic Fe52, Fe53, and Hβ in the range of evolutionary parameters pertinent to elliptical galaxies and globulars, and comparison was made with the whole available set of observations constraining the elemental partition in the current chemical mix of these stellar systems. Briefly, these are the main points results of our analysis.

(i) Fe52 and Fe53 indices revealed to be unbiased and direct indicators of the iron content in a SSP. Their dependence on the location of the HB as well as of bright giants in the RGB and AGB is found to be weak, and the integrated indices are not sensibly affected by details in stellar mass loss. In metal-rich populations they are mainly contributed by stars at the base of the RGB.

(ii) Hβ revealed to be an effective tracer of the temperature distribution of stars in the upper MS and SGB, allowing us therefore to test the temperature of the turnoff point in a SSP. Response to a bluer morphology of the HB (IHB in the Buzzoni 1989 notation) is however large, and in the sense of increasing the index of 0.7 Å with respect to the RHB case. Since the metallicity dependence of Hβ mainly derives from temperature effects on the turnoff region, the comparison with the globular cluster observations led us to conclude that standard isochrones older than 18–20 Gyr would be required to fit the data or, alternatively, the light α elements should be enhanced in 15 Gyr SSPs. The latter hypothesis would better fit with the observational evidences for oxygen enhancement in Population II stars of the Galaxy from high-resolution stellar spectroscopy.

(iii) Concerning iron and magnesium, [Mg/Fe] is found in average solar but a systematic residual trend of observations respect to models is evident. The sense is that at high metallicity iron is deficient respect to magnesium. On the basis of the comparison with the models we concluded that the Fe abundance (per unit mass) in the galaxies is constant. This result might pose important constraints on the chemical history of early type galaxies with a special concern on the SN rate and the induced metal enrichment.

The unified scenario leading to a substantially similar genesis for both stellar populations in globular clusters and elliptical galaxies is therefore supported by our results. Globulars might have been partially enriched in their early evolution by SNe II which supplied the excess of light α elements in the chemical mix. On the contrary, ellipticals were massive enough to retain with better efficiency SN II ejecta, and also to experience SN I events progressively supplying iron.

The SN I enrichment should have proceeded in a similar way in galaxies with different total mass such as to end up with a constant Z_{Fe} throughout, while CNO elements should have mainly accumulated in giant ellipticals thanks to a less dramatic gas stripping during the early SN-driven wind phase envisaged by theory. This might account thus for the currently observed trends between [Mg/Fe] and [Fe/H].

It is a pleasure to acknowledge enjoyable interactions with many colleagues, who contributed with stimulating ideas and suggestions. We thank Jim Rose, the referee, for his competent review of the original version of the paper. Sandy Faber supplied part of the Gorgas *et al.* (1993) data in real time. Thanks for her kindness and efficiency. Guy Worthey kept us posted on his Ph.D. work, that much dealt with some of the problems addressed in this paper. Finally, many thanks to Luciana Federici and Flavio Fusi Pecci, for providing us with the unpublished spectra of the M31 clusters shown in Fig. 15.

REFERENCES

Aaronson, M., Cohen, J. G., Mould, J., & Malkan, M. 1978, ApJ, 223, 824
Aaronson, M., Frogel, J. A., & Persson, S. E. 1978, ApJ, 220, 442
Arimoto, N. 1988 in Towards Understanding Galaxies at Large Redshift, edited by R. G. Kron and A. Renzini (Kluwer, Dordrecht), p.43
Arimoto, N., & Yoshii, Y. 1987, A&A, 173, 23
Baldwin, J. R., Danziger, I. J., Frogel, J. A., & Persson, S. E. 1973, ApJ, 14, 1
Baldwin, J. R., Frogel, J. A., & Persson, S. E. 1973, ApJ, 184, 427
Battistini, P., Bonoli, F., Braccesi, A., Federici, L., Fusi Pecci, F., Marano, B., & Borngen, F. 1987, A&AS, 67, 447
Bergbush, P. A., & VandenBerg, D. A. 1992, ApJS, 81, 169
Bessell, M. S., Sutherland, R. S., & Ruan, K. 1991, ApJ, 383, L71
Boulade, O., Rose, J. A., & Vigroux, L. 1988, AJ, 96, 1319
Brodie, J. P., & Huchra, J. P. 1990, ApJ, 362, 503
Buonanno, R., Corsi, C. E., & Fusi Pecci, F. 1989, A&A, 216, 80
Burstein, D., Bertola, F., Buson, L., Faber, S. M., & Lauer, T. R. 1988a, ApJ, 328, 440
Burstein, D., Faber, S. M., Gaskell, C. M., & Krumm, N. 1984, ApJ, 287, 586
Buzzoni, A. 1989, ApJS, 71, 817
Buzzoni, A. 1993, A&A, 275, 433
Buzzoni, A., Gariboldi, G., & Mantegazza, L. 1992, AJ, 103, 1814 (Paper I)
Cayrel de Strobel, G., Bentolila, C., Hauck, B., & Duquennoy, A. 1985, A&AS, 59, 145
Cayrel de Strobel, G., Hauck, B., François, P., Thévenin, F., Friel, E., Mermilliod, M., & Borde, S. 1992, A&AS, 95, 273
Chieffi, A., Straniero, O., & Salaris, M. 1991 in the Formation of Star Clusters, edited by K. Janes, ASP Conf. Ser., 13, 219
Dickow, P., Gyldenkerne, K., Hansen, L., Jacobsen, P. U., Johansen, K. T., Kjaergaard, P., & Olsen, E. H. 1970, A&AS, 2, 1
Faber, S. M. 1973, ApJ, 179, 731
Faber, S. M., & Franch, H. 1980, ApJ, 235, 405
Faber, S. M., Friel, E. D., Burstein, D., & Gaskell, C. M. 1985, ApJS, 57, 711
Ferrini, F., & Poggianti, B. 1993, ApJ, 410, 44
Frogel, J. A. 1985, ApJ, 298, 528
Frogel, J. A., Persson, S. E., Aaronson, M., & Matthews, K. 1978, ApJ, 220, 75

© American Astronomical Society • Provided by the NASA Astrophysics Data System

1994AJ....107..513B

Frogel, J. A., Persson, S. E., & Cohen, J. G. 1980, ApJ, 240, 785
Fusi Pecci, F., & Renzini, A. 1978 in The HR Diagram, IAU Symposium No. 80, edited by A. G. D. Philip and D. S. Hayes (Reidel, Dordrecht), p. 225
Gorgas, J., Efstathiou, G., & Aragon Salamanca, A. 1990, MNRAS, 245, 217
Gorgas, J., Faber, S. M., Burstein, D., Jesus Gonzalez, J., Courteau, S., & Prosser, C. 1993, ApJS, 86, 153
Gratton, R. 1992, MSAIt, 63, 173
Greggio, L., & Renzini, A. 1983a, A&A, 118, 217
Greggio, L., & Renzini, A. 1983b, MSAIt, 54, 311
Hansen, L., & Kjaergaard, P. 1971, A&A, 15, 123
Johnson, H. L. 1966, ARA&A, 4, 193
Kurucz, R. 1979, ApJS, 40, 1
Kurucz, R. 1992, in The Stellar Populations of Galaxies, edited by B. Barbuy and A. Renzini (Kluwer, Dordrecht), p. 225
Matteucci, F. & Brocato, E. 1990, ApJ, 365, 539
Matteucci, F., & Greggio, L. 1986, in Nucleosynthesis and its Implications on Nuclear and Particle Physics, edited by J. Audouze and N. Mathieu, NATO-ASI Series, 163, 315
Reid, N., & Mould, J. 1985, ApJ, 299, 236
Renzini, A. 1977, in Advanced Stages in Stellar Evolution, edited by P. Bouvier and A. Maeder (Geneva Observatory, Geneva), p.149
Renzini, A., & Buzzoni, A. 1986, in Spectral Evolution of Galaxies, edited by C. Chiosi and A. Renzini (Reidel, Dordrecht), p. 195
Rose, J. A. 1984, AJ, 89, 1238
Rose, J. A. 1985a, AJ, 90, 787
Rose, J. A. 1985b, AJ, 90, 803
Rose, J. A. 1985c, AJ, 90, 1927
Rose, J. A., & Tripicco, M. J. 1984, ApJ, 285, 55
Saito, M. 1979, PASJ, 31, 181
Sneden, C., Kraft, R. P., Prosser, C. F., & Langer, G. E. 1991, AJ, 102, 2001
Spinrad, H., & Taylor, B. J. 1969, ApJ, 157, 1279
Spinrad, H., & Taylor, B. J. 1971, ApJS, 22, 445
Straniero, O., Chieffi, A., & Salaris, M. 1992, MSAIt, 63, 43
Taylor, B. J. 1970, ApJS, 22, 177
Taylor, B. J. 1991, ApJS, 76, 715
Trimble, V. 1991, ARA&A, 3, 1
VandenBerg, D. A. 1983, ApJS, 51, 29
VandenBerg, D. A. 1992, ApJ, 391, 685
Wheeler, J. C., Sneden, C., & Truran, J. W. 1989, ARA&A, 27, 279
Worthey, G. 1992, Ph.D. thesis dissertation, University of California
Worthey, G., Faber, S. M., & Jesus Gonzalez, J. 1992, ApJ, 398, 69
Zinn, R., & West, M. 1984, ApJS, 55, 45

© American Astronomical Society • Provided by the NASA Astrophysics Data System